Monte Carlo modeling of radio-frequency breakdown in argon

Marija Puač[1, 2], Dragana Marić[2], Marija Radmilović-Radjenović[2], Milovan Šuvakov[2] and Zoran Lj. Petrović[2, 3]

[1]*also at: Faculty of Electrical Engineering University of Belgrade*

[2]*Institute of Physics, University of Belgrade, Pregrevica 118, 11080 Zemun, Serbia*

[3]*also at: Serbian Academy of Sciences and Arts, Knez Mihailova 35, 11001 Belgrade Serbia*

This paper contains results of the detailed simulation study of the breakdown in low-pressure radio-frequency argon discharges. Calculations were performed by using a Monte Carlo code including electrons only, assuming that the influence of heavy particles is negligible. The obtained results are in a good qualitative agreement with the available experimental data and clearly show multivalued nature of the left-hand branches of the breakdown voltage curves. Physical processes defining the breakdown conditions are analyzed based on the spatial profiles of electron density, local mean energy, number of elastic and ionization collisions. Under conditions where two breakdown values exist one could identify two regimes and two different balances between electron losses and production. From the dependence of the breakdown voltage on the product of the pressure and the interelectrode distance and frequency over the gas number density, similarity laws for radio-frequency breakdown have been reexamined.

1. Introduction

Capacitively coupled radio-frequency (RF) discharges are attracting an increased attention due to their wide applications in many technological processes [1] such as plasma etching for semiconductor materials, thin film deposition, plasma cleaning [2] and increasingly popular biomedical applications [3-5]. One of the crucial issues is understanding the pertinent processes that drive the breakdown and transition to RF plasma and how those could be modeled. In that respect a wealth of information can be obtained from the breakdown voltage curves. Gas breakdown represents the first step in plasma generation. Specific characteristic of RF plasmas is that the self-sustained discharge may be maintained merely through ionization by electrons. There, the feedback process is the return of electrons when field changes direction as a replacement of the ion drift towards the cathode that is the feedback in DC discharges [6-9].

Although, gas breakdown has been studied for more than 100 years, many aspects are poorly understood, even at the present day. A simplified explanation dating back to the early version of the textbook by von Engel [8] (and perhaps even deeper in the past) is that only the group of electrons that completes the transition in one half period from one electrode to the other has a

chance of being multiplied. Basically, the drift velocity integrated and averaged over the half period has to be equal to the gap between two electrodes [6,7]. In the first half of the 20th century there has been a major development of techniques to solve time dependent Boltzmann equation [10-16] continued by Wilhelm and Winkler in 70s and Makabe in 80s [17,18]. First exact solutions for the time dependent transport have been obtained by using Monte Carlo (MC) simulations [19] and numerical solutions to the time dependent Boltzmann equation [20,21]. Numerous approximate experimental and theoretical papers have been published on breakdown in RF using simplified semi-analytic forms [22-26]. At the same time fluid, hybrid and Particle in Cell (PIC) models of RF plasmas include the early stages of the growth of ionization [18, 27, 28]. In recent years, computer modeling and simulation has emerged as an effective tool that complements laboratory experiments and analytic models. Particle-in-cell/Monte Carlo (PIC-MC) simulations have been used extensively to study fundamental processes in capacitively coupled RF discharges [29- 32].

As it has been mentioned earlier, that electrons alone may maintain discharge through ionization and describe the main features of the breakdown curves we start from electrons as the only agents precipitating the breakdown. Only after we start comparing with experiment we shall add other effects (ion induced secondaries, metastable induced secondaries, fast neutrals and their effect, photon induced secondaries and finally electron induced secondaries-multipactors). But those are not in the scope of this paper. In this paper calculations were performed for argon discharges by using a Monte Carlo code under condition of the low degree of ionization so that the transport of particles takes place in the externally defined uniform field. In doing so we tried to take the advantage of the well tested Monte Carlo codes that may provide very accurate time dependent transport data [33, 34]. At the same time development of the plasma through weakly ionized phases in order to test the applicability of transport coefficients and fluid models in representing such breakdown. Thus, we have used a fully tested and benchmarked code for electrons (that also has a facility to include heavy particles, ions and neutrals) with a full range of sampling and treatment of the cross section data. The logic is that during the breakdown the swarm physics describes exactly the charged particle ensemble and only a much higher densities one needs to include the space charge effects. This paper represents one of the first steps in obtaining a more complete description of the low-pressure RF argon discharge which provides us with an insight into the basic physics of the breakdown (preliminary results were presented in [35]).

2. Methods

For this study a Monte Carlo (MC) code developed and tested (tested both for DC and RF benchmarks [33, 34]) is used. Since Monte Carlo technique has been explained elsewhere [37, 38], only a brief description of the code will be given here. We developed MC code that traces electrons only. Heavy particles and the effect of photons may also be added, but those results are

not included in this paper. The code has been tested for electrons (and ions) transport and was shown to give accurate electron energy distribution functions and transport coefficients in model gases and in argon [33, 37].

Calculations were carried out for argon discharges generated between infinite plane-parallel electrodes at frequency of 13.56 MHz (unless specified otherwise). Argon is chosen for many reasons: first of all, it is an atomic gas with simple energy transition spectrum and it is easy to operate with it. At the same time, cross section data and other necessary input data are available and well tested, thus are reliable. One can refer to argon as a "benchmark" gas in discharge studies. The set of cross sections for electron scattering on argon includes elastic, ionization and two excitation cross sections that have been well tested for argon swarms [39, 40].

At the beginning, electrons have been released from the middle of the gap between the two electrodes with no initial energy. Any further electron motion and different interactions depend on the applied alternating current (AC**)** field, random number generator and solutions of kinetic and balance equations. At this point, surface effects at the electrodes are not included. When an electron reaches the boundary, it is assumed to be removed and has no influence on discharge kinetics. We have a facility to add reflection or other surface processes easily based on the available experimental data.

In our simulations the breakdown voltage curves were recorded in accordance with the procedure described in [6, 41, 42]. On the right-hand side of the breakdown voltage curve, the breakdown voltage was determined by fixing a pressure and increasing the applied voltage. For the left hand side of the curve, the voltage was fixed while the pressure was varied. In Monte Carlo simulations these two procedures are equally simple while in case of experiments variation of the pressure may be more complex.

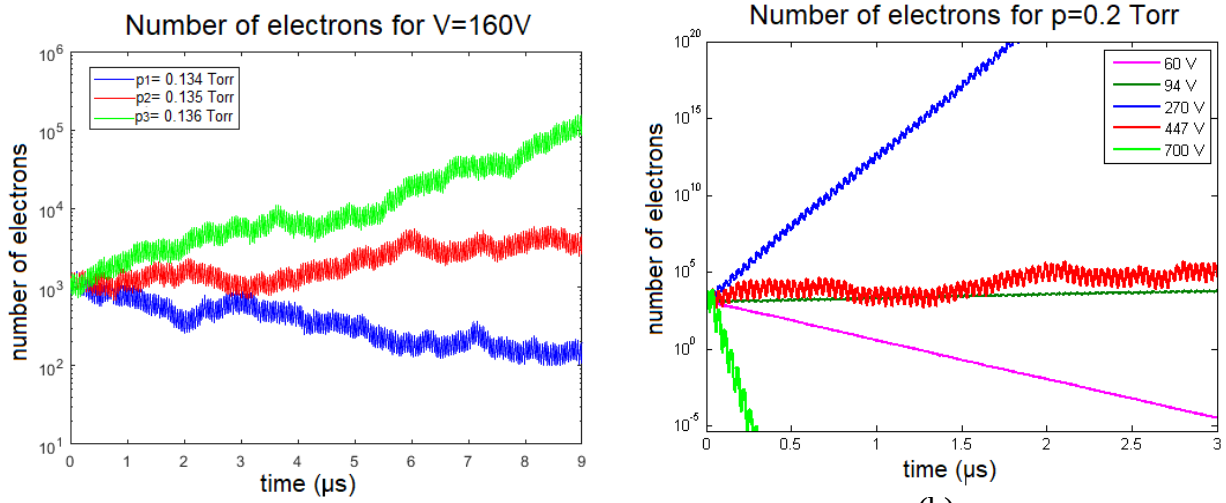

Figure1: The time dependence of the simulated number of electrons for: a) the fixed voltage of 160 V and various pressure and b) constant pressure of 0.2 Torr and various voltages.

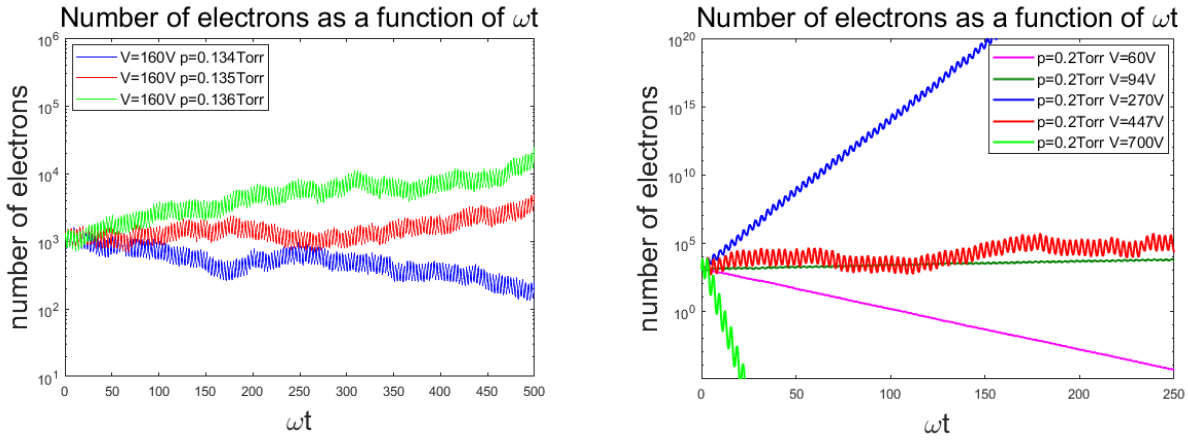

(a) (b)

Figure1: The time dependence of the simulated number of electrons for: a) the fixed voltage of 160 V and various pressure and b) constant pressure of 0.2 Torr and various voltages.

Figure1 shows changes of numbers of electrons over time for: a) the fixed maximum voltage of V=160 V and at three different pressures (p_1=0.134 Torr, p_2=0.135 Torr and p_3=0.136 Torr) and b) the fixed pressure of 0.2 Torr and five different voltages (60 V, 94 V, 270 V, 447 V and 700 V). As can be seen from Figure 1a, at the pressure p_1 there is no electron amplification in the required quantity that can compensate the electron losses at the electrode, so the total number of electrons decreases over time and the slope is negative. At the pressure p_2, however, there is a notable increase in total number of electrons over time, which can be interpreted as an increased number of ionizations due to the higher density (as compared to p_1) of background atoms and consequently a larger number of collisions. Breakdown occurs somewhere between p_1=0.134 Torr and p_2=0.135 Torr. The pressure resolution was 0.001 Torr. A more accurate pressure can be obtained by interpolation between the nearest two values of pressure, in this case p_1 and p_2.

Figure 1b is presented to depict how number of electrons in time changes with large variations of voltages. Pressure (0.2 Torr) and voltages that are chosen correspond to vertical line in Figure 2a (but not the numbers).When pressure is fixed (see Figure 1b), there are two values where mean number of electrons is barely maintained which means that those are the boundaries of the breakdown (94 V and 447 V). In-between the two breakdown values one has excessive growth of the density (that would in real circuit push the operating point to either of the two breakdown voltages). Result within that range have a positive slope results outside that range show decay advancing towards termination (e.g. data for 60 V and 700 V). Outside the breakdown region (above 447 V and below 94 V) the density of electrons rapidly diminishes (60 V and 700 V).

In both Figures, 1a and 1b, there are periodic oscillations of the electron number. In Figure 1a, with fixed voltage, these oscillations are the same in sense of the period and amplitude. In Figure 1b period of oscillations is the same while amplitudes are different depending on applied voltage. With changes in voltage the effective rates that define the speed of relaxation may change and

affect the undulations of the properties such as number of electrons. For high voltage electrons reach ionization energies more easily and in larger numbers so the number of electrons changes more rapidly within one period of time. Losses at electrodes may balance the increased production, they are increased because more of electrons are being pushed to the electrodes by strong AC field. As voltage is decreasing less energy is transferred from the field to electrons and number of ionizations is reduced (increase of number of electrons within one period is smaller). For lower voltage both losses and production are smaller as electrons do not reach electrodes (oscillation are barely noticeable for voltage of 60 V). One can conclude that period of oscillation of electron number is determined by the frequency of external AC field while the amplitude of oscillation of electron number depends on amplitude of applied AC field (energy transfer from field to electrons).

3. Results and Discussion

3.1. Spatial profiles of electron density and ionization rate as representation of a potential for achieving breakdown

The dependence of the RF breakdown voltage on the pressure is presented in Figure 2. Results of our MC simulations (red circles) are compared with the experimental data taken from ref. [6] (blue squares) in Figure 2a. As can be seen on the left-hand side of the simulated curve, for a fixed pressure there are two values of the breakdown voltage. Discharge may start between these two values, while above and below it quenches rapidly (as indicated in Figure 1). This observation is in agreement with the previously published experimental data [6], at least qualitatively. Crosses correspond to the sampling points on a vertical line p=0.2 Torr. Two points are on the breakdown curve (94 V and 447 V) and two points are in-between (170 V and 300 V). In principle, in simulations operation above the breakdown conditions, and thereby the growth of electrons, is allowed. In experiments, however, the operating point will move towards either of the two breakdown curves. Development of spatial profiles (see Figure 3, 4) along the vertical line provides an insight into the pertinent physical processes. On the other hand in Figure 2b sampling points marked by letters are on the breakdown curve. The spatial profiles associated with these points and shown in Figure 5 indicate difference in physical processes with variation of p (pd).

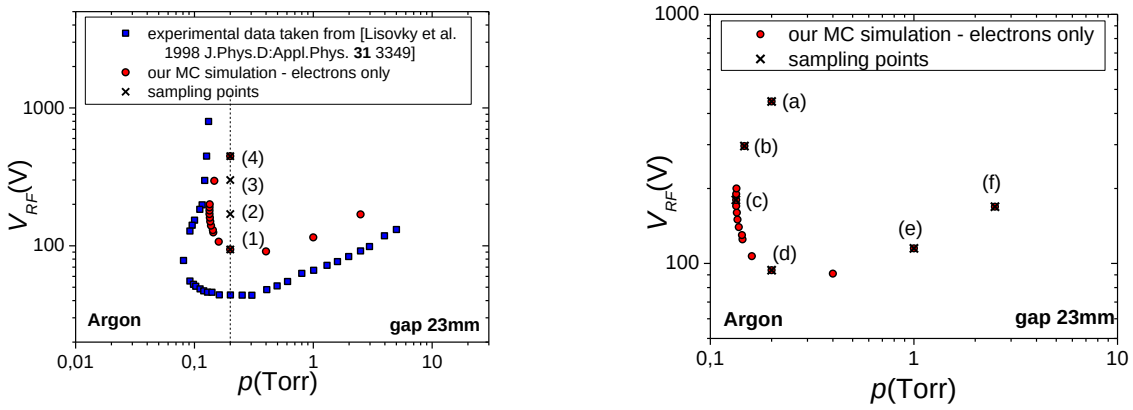

(a) (b)

Figure2: The breakdown voltage curves for argon RF discharges at 13.56 MHz and the gap size of 23 mm. The MCS includes electrons only. a) Comparison of the breakdown voltage curve obtained by MCS (red circles) and experimental available data [6] (blue squares). Vertical line for p=0.2 Torr and different voltages indicates sampling points presented in Figures 3 and 4. b) MCS obtained curve indicating sampling points of spatial profiles presented in Figure 5. Sampling points are marked by numbers and letters.

Spatio-temporal development of profiles of: electron density, mean energy, elastic collisions and ionization are shown in Figure 3. Calculations were performed for the frequency of 13. 56 MHz, the gap size of 23 mm, the pressure of 0.2 Torr and two breakdown points: a) 94 V and b) 447 V (as indicated in Figure 2a). As voltage increases, the low voltage breakdown point is reached, but most of the electrons do not reach the electrodes. The profile of the electron cloud is broad, not really sinusoidal, but generally follows a sinusoidal shape. There are maxima in density, elastic scattering and in mean energy when cloud is closest to the electrodes. Peaks are delayed by a large phase delay to the voltage waveform. In fact, the peak starts moving towards the center of the gap only at the phase when the field changes direction and not for the maximum of the field. This can be easily understood. As for ionization only two regions close to the maximum of the applied voltage (field) are abundant in collisions while still following a similar temporal and spatial dependence.

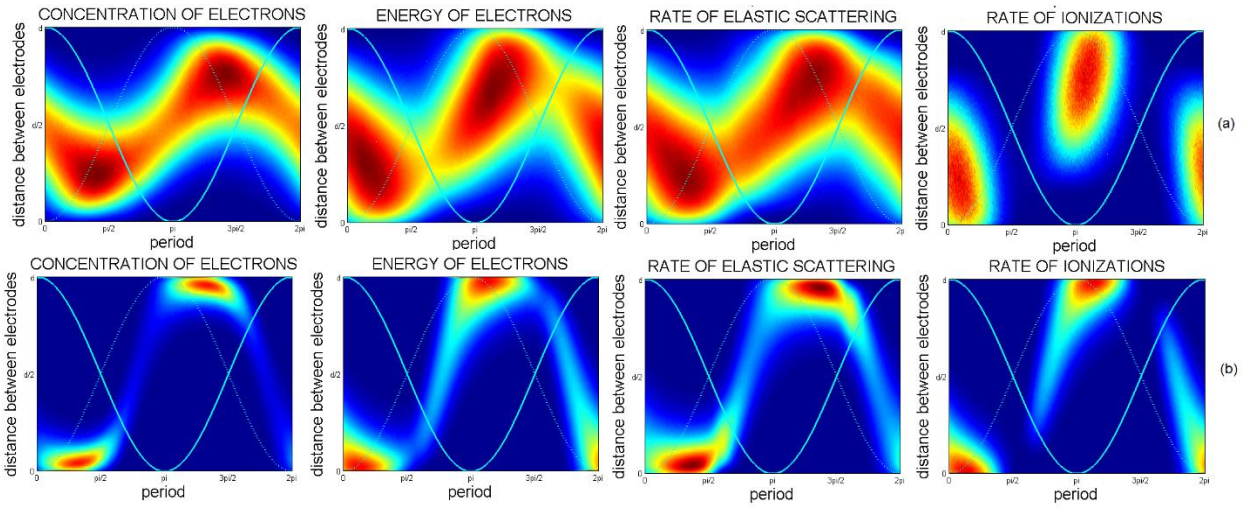

Figure3: Spatial distributions of: electron concentration, mean energy and rates of elastic scattering and ionization for the pressure of 0.2 Torr and two breakdown points: (a) V=94 V and (b) V=447 V (points are marked in Figure 2a, (a) corresponds (1) and (b) corresponds (4)). Light blue line represents AC field, while dashed light blue line corresponds to the field dependence inverted to represent the force affecting the electrons. Interelectrode gap is 23 mm and frequency is 13.56 MHz. Number of electrons in the simulation was selected to have a similar statistical quality of the results with the smallest rate (i.e. ionization). Thus the colour scales are not representing any quantitative data that may be compared for different conditions only the indication of the profile of the ensemble.

At the higher breakdown point the spatial profiles are much narrower and there is a strong overlap with the electrode. While electron density peaks are slightly away from the electrode the highest energy/the most likely to ionize electrons peak is right at the edge of the electrode.

It is important to note that our MC code obtains a double valued voltage on the breakdown curve by treating electrons only. For some gases [43] even “S” shaped curves with three points may be observed. Explanation of this phenomenon can be the following. For the lower voltage one needs to compensate losses at electrodes by increasing ionization, and any increase in voltage leads to a higher ionization. If we move to higher voltages, ionization is increased but so are the losses at the instantaneous anode. This is a consequence of pushing electrons closer to electrodes by an increasing AC field. The losses may be represented by imagined remaining electron ensemble spatial distributions that extends over the electrode edge into its bulk and this distributions increase with the applied voltage. At a certain point this part of the ensemble that passes past the electrode will increase so much that ionization in gas (in front of the electrode) cannot compensate the losses and discharge will switch itself off. In Figure 3 this is represented by the spatial profile of electron concentration and mean energy which indicates a potential for ionization.

The profile of the increasing ionization rate of the group closest to the anode is shown in Figure 4 along the fixed p= 0.2 Torr for four points marked in Figure 2a. With an increasing voltage

more and more of the ionization capable electrons would be lost at the surface. At the lower applied voltage (94 V) though, the swarm oscillates between two electrodes without reaching them and majority of ionization capable electrons have no difficulty to ionize.

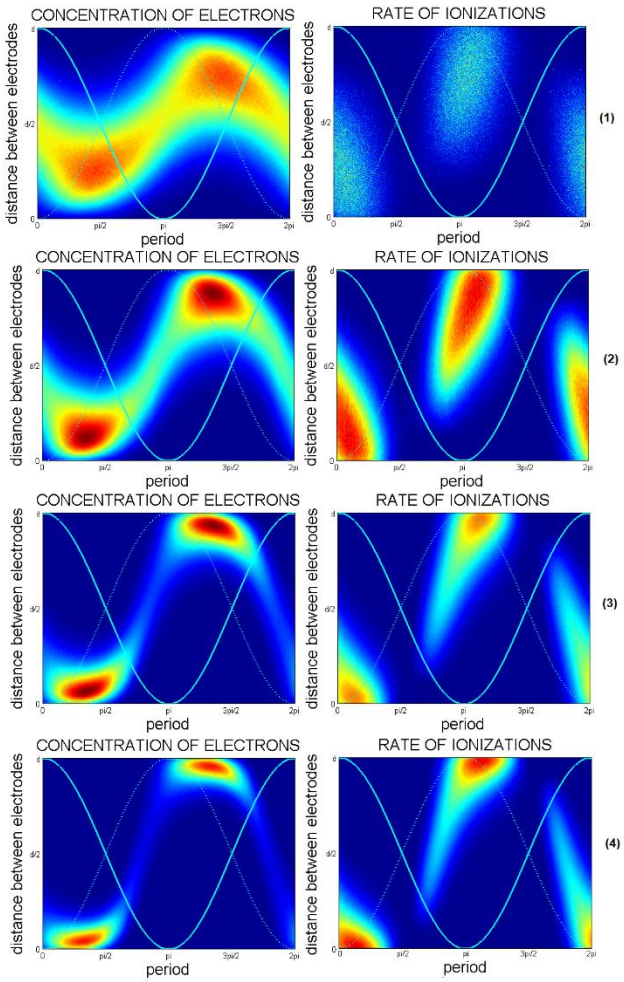

Figure 4: Spatial profiles of the electron concentration and ionization rates for the pressure of 0.2 Torr and voltages of (1) 94 V, (2) 170 V, (3) 300 V and (4) 447 V. Points are marked in Figure 2a. Interelectrode gap is 23 mm and frequency is 13.56 MHz. All figures are obtained with the same initial number of electrons so the relative magnitudes of the same coefficient are indicated by the colors scale.

3.2. Variation of the spatial profiles with *pd* along the breakdown curve

Having presented results that indicate the changes in the spatial profiles of all the discharge parameters along a vertical line (p=const.), Figure 5 exhibits the spatial profiles along the Paschen-like breakdown potential curve. Stating that the curve is Paschen-like does not imply in any way that Paschen mechanism is relevant here in its entirety. The points on V- p plane that

have been selected to show the spatial profiles of various properties of the electron swarm ensemble are marked on the breakdown curve shown in Figure 2b.

Plots (a) and (d) in Figure 5 are repeated from the previous figures. The first represents the higher point on the breakdown curve, the second the lower point on the breakdown curve for p= 0.2 Torr. Plots (b) and (c) are on the left rapidly rising branch of the breakdown curve. It is clear that under those conditions the magnitude of the field manages to bring all of electrons in the immediate neighborhood of the electrodes during one half period. Those points have all the characteristics of the operation well above the lower breakdown points and close to the upper branch. The principal issue here is whether the losses at the electrode may be balanced by the production of electrons in its proximity, the production that is made more and more difficult by the reduced number of collisions in a similar fashion to the left hand branch of the DC Paschen curve. As a result of this balancing between losses and gains the peak of the mean energy and the number of ionizing collisions clearly occur right before reaching the electrode and after the maximum in the field. At the same time peak in density occurs a little later as a consequence of the ensuing burst of ionization. Number of elastic collisions follows the profile of density better, while, as stated, number of ionizations follows the profile of the mean energy.

Spatial profiles in Figure 5c also become somewhat closer to the lower branch profiles of the Figure 5d, where majority of ionizations occur in the bulk of the discharge, and the whole ensemble merely brushes against the electrodes. The balance between losses and gains, as displayed in Figure 5d seems optimal as there are minimal losses while the number of collisions provides ample opportunities to compensate for them. As pressure increases (for a fixed d) the number of collisions increases further and thus it is more difficult to achieve higher energies so the breakdown voltage increases but slowly. More importantly, the density profile of electrons loses sharp peaks and becomes more sinusoidal in the center of the gap with vanishing density due to losses close to the walls. Mean energy is still modulated following the field dependence albeit with a delay. A similar modulation is observed in elastic collisions mainly due to the energy dependence of the cross section. It is important to note that collisions occur on both halves of the gap, as the density profile, while modulated, does not show complete migration of electrons towards the instantaneous anode and away from the cathode. As a result of the ensemble overlapping from one to the other electrode, the highest energy electrons responsible for ionization will be generated throughout the gap and under those conditions, ionization, however weak, spreads on both halves almost equally (Figure 5e, 5f). The difference between ionization profiles in Figure 3a and Figure 5d is that in the former one we have enhanced the number of events by accumulation of events through releasing more electrons for the same set of conditions to make the simulation conditions the same for all figures in the cluster Figure 5.

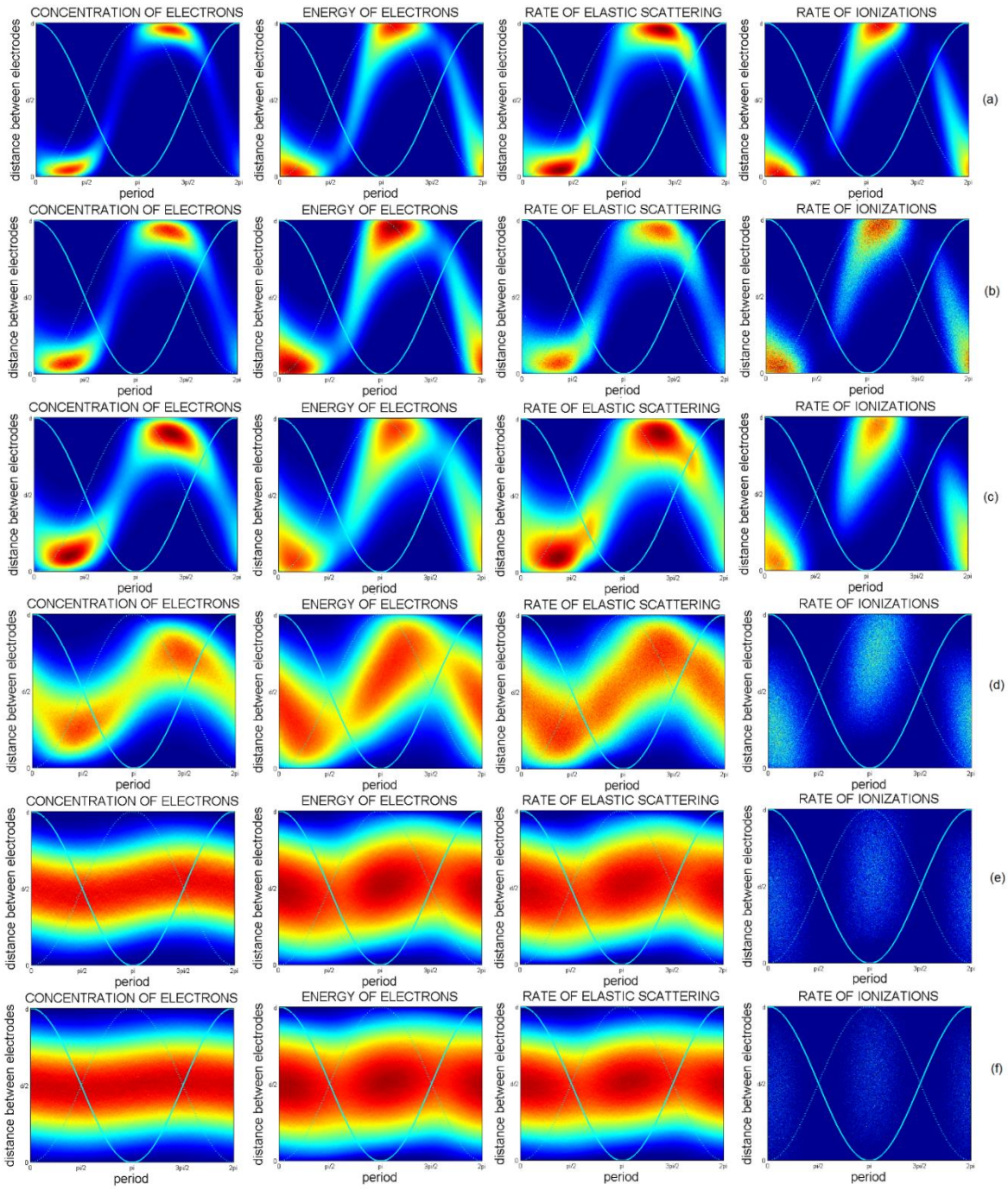

Figure 5: Spatial distributions of concentration of electrons, electron energy and rates of elastic scattering and ionization: (a) 447V 0.2Torr, (b) 296V 0.147Torr, (c) 180V 0.1335Torr, (d) 94V 0.2Torr, (e) 115V 1Torr and (f) 169V 2.5Torr. Points are marked in Figure 2b. Interelectrode gap is 23 mm and frequency is 13.56 MHz. All figures are obtained with the same initial number of electrons so the relative magnitudes of the same coefficient are indicated by the colors scale.

Furthermore, we can employ the Monte Carlo code to provide us a more detailed picture of physical processes by observing the energy distribution function that has to be related to the

processes occurring in the region of active ionization (i.e. near the electrode). As can be seen in Figure 6, the overlap of the distribution function with the relevant cross sections (both excitation of metastable and ionization) may be of significant importance for the maintenance of the discharge. For high voltages (Figure 6a) there is a significant overlap of EEDF and cross section for ionization. A great deal of high energy electrons that can ionize are being absorbed by electrodes and lost. At this conditions (V=447 V and p=0.2 Torr) there is a fine balance between losses and production of electrons. As voltage increases, more of the high energy electrons would be lost at electrodes and discharge cannot be maintained (double valued nature of RF breakdown curve occur). A significant increase of the EEDF right in front of the electrode at higher voltages (i.e. lower pressures) also can be observed. The increased mean energy for lower pressures is the result of a reduced number of collisions as electrons cross the gap so ionization has to become more efficient. As for high pressures (Figure 6b) only tail of EEDF at electrodes is being overlapped with cross section for ionization. There is no significant loss of ionization capable electrons and discharge is easier to maintain which can be observed as smaller increase of voltage in right branch of breakdown voltage curve comparing with the left branch.

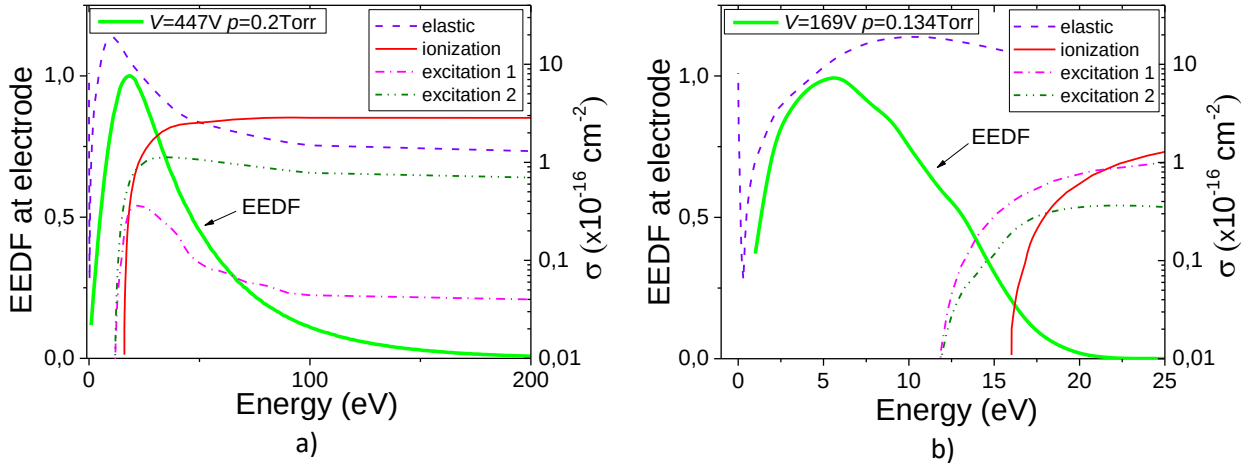

Figure 6: Electron Energy Distribution Function (EEDF) at the electrodes separated by 23mm at the frequency of 13.56MHzfor: (a) U=447V, p=0.2Torr and (b) U=169V, p=2.5Torr. Right hand side *y*-axes shows set of cross sections for argon.

3.3. Scaling of RF breakdown profiles: Breakdown voltage depending on the gap length and frequency

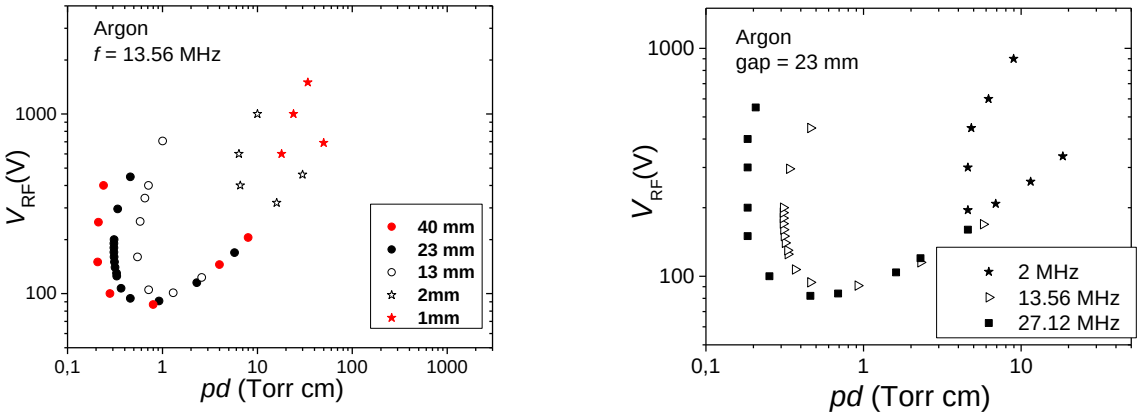

(a) (b)

Figure 7:a)Simulated breakdown voltage curves for: a) a fixed frequency of 13.56 MHz and various gaps sizes and b) a fixed gap of 23 mm and various frequencies.

RF breakdown has a different nature comparing to DC breakdown. Therefore, *pd* scaling that is applicable in DC breakdown voltage curves needs to be extended to include frequency dependence. Figure 7 shows breakdown voltage curves for various: a) gaps and b) frequencies. The curves have a similar shape with a large variation of parameters. For a fixed frequency one cannot maintain the scaling, as in addition to *pd* scaling there is also *fd* (interelectrode distance times frequency) scaling that needs to be satisfied [44, 45]. The same is valid for a fixed gap. Scaling with proper variation of both frequency and the gap is shown in Figure 8.

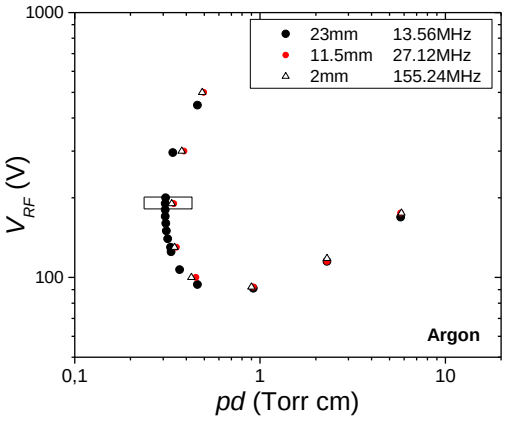

Figure 8: Scaling according to *pd* and *fd* scaling laws of RF voltage breakdown curves. Box indicates region with points for which the spatial profiles are plotted in Figure 9.

Both frequency and gap are varied while keeping the *fd* constant and observing the *pd* dependence. We can see a very good overlap that is excellent at higher *pd* while at lower *pd* and higher breakdown voltages there is more difference presumably due to nonlinearities brought about by the overlap of the electron cloud with the electrode. While presenting a breakdown curve scaling is important and indeed points out the validity of the scaling. The critical test of the scaling would be the observation of the spatial profiles depicted in Figure 9 for *pd* around 0.34 Torr cm and a number of frequencies with the corresponding gaps. It is clear that for a narrow range of *fd* and *pd* all spatial profiles coincide. That is the physical foundation of the scaling laws which basically scales the number of collisions per length and in time.

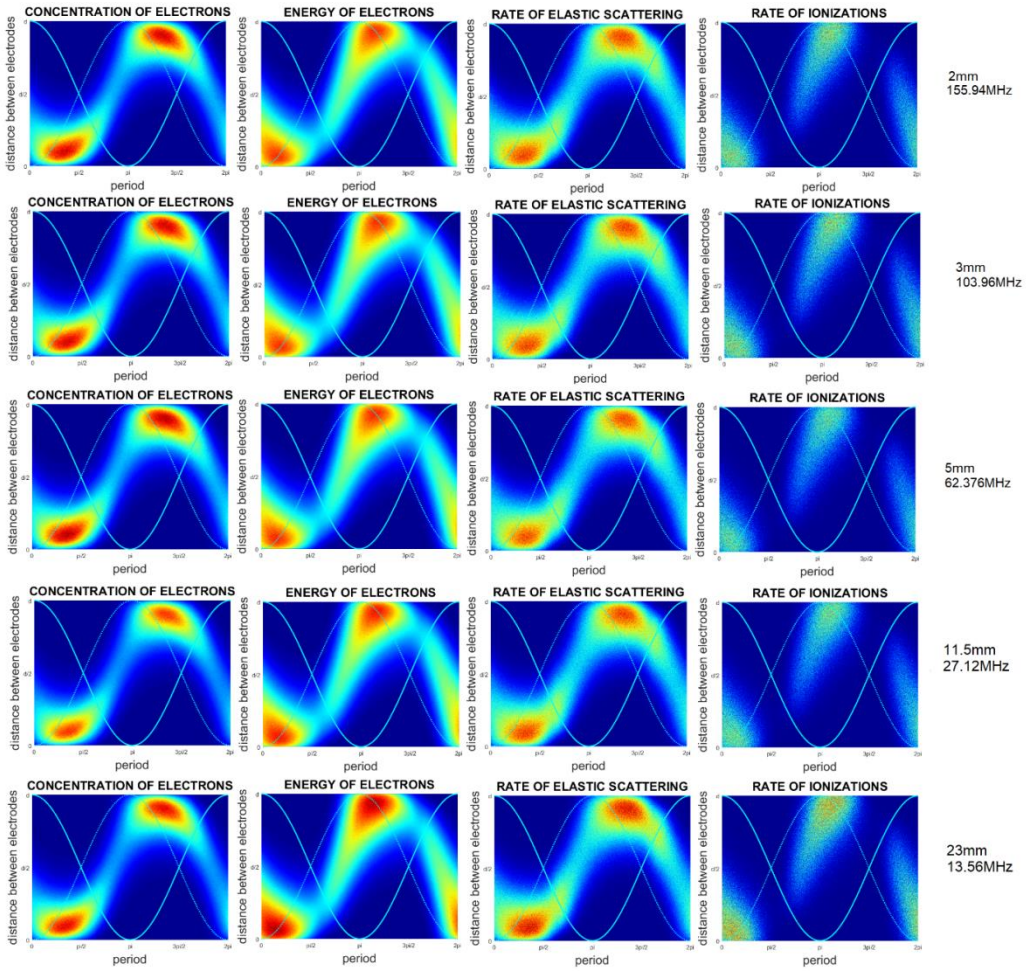

Figure 9: Spatial distributions for a number of points that have the same product of *f* and distance between electrodes (*fd* =constant) and also for a fixed *pd*=0.34 Torr cm. All figures are obtained with the same initial number of electrons so the relative magnitudes of the same coefficient are indicated by the colors scale.

4. Conclusion

In this paper physical background of the low-pressure RF argon discharges is studied. It is found that the simplified phenomenology of transfers from one electrode to the other is often not met especially at higher pressures where electrons may produce sufficient ionization while crossing shorter distances. At lower pressures, conditions to reach the electrodes are acquired at the cost of an increased breakdown voltage. Under those conditions the balance between produced new electrons and the increase in mean energy determines the breakdown. Thus it is possible to have two breakdown points (and the region of the double valued breakdown curve coincides with the region where electrons reach electrodes in one half period) for one *pd* value. The higher point is where balance is encountered due to losses of high energy electrons hitting the anode and being absorbed by it.

Another issue of scaling is illustrated well with the obtained results. The breakdown follows the standard *pd* scaling very well but it has to adjust itself to the ω/N scaling as well. The *fd* scaling has been discussed within the terms of breakdown physics by Lisovsky et al [45] and it was addressed to the reference [44]. However both scalings have been established in the earlier electron transport (swarm) studies [14-16] basically as a condition to maintain the number of collisions per certain distance or in certain time. The spatial profiles of electron properties shown in Figure 9 give an indication of how scaling involves identical spatial distributions and other properties thus supporting the predicted scaling.

Results, presented and discussed here, confirm that modeling of RF breakdown by using a detailed MC code provides an excellent and relatively easy entrance into the pertinent physical processes. In later stages plasma properties become important and one has to follow the space charge development which makes the situation much more complex. Yet the onset of the breakdown is purely a swarm phenomenon and the beginning of the development of the plasma may be clearly envisioned and explained even quantitatively by a swarm model.

Acknowledgement: This paper was completely finalized at the Institute of Physics University of Belgrade under the basic funding through projects OI 171037 and III 41011 of the Serbian Ministry of Education, Science and Technological development of Serbia. ZLjP is grateful to Serbian Academy of Sciences and Arts and its project F155 for its partial support. Authors are grateful to Dr Srđan Marjanović for help in several stages of the development of the code.

[1] Adamovich I, Baalrud S D, Bogaerts A, Bruggeman P J, Cappelli M, Colombo V, Czarnetzki U, Ebert U, Eden J G, Favia P, Graves D B, Hamaguchi S, Hieftje G, Hori M, Kaganovich I D, Kortshagen U, Kushner M J, Mason N J, Mazouffre S, Mededovic Thagard S, Metelmann H-R, Mizuno A, Moreau E, Murphy A B, Niemira B A, Oehrlein G S, Petrovic Z Lj, Pitchford L C, Pu Y-K, Rauf S, Sakai O, Samukawa S, Starikovskaia S, Tennyson J, Terashima K, Turner M M, van de Sanden C M M and Vardelle A 2017 *J. Phys. D: Appl. Phys*. **50** 323001

[2] Makabe T and Petrović Z Lj 2006 *Plasma Electronics: Applications in Microelectronic Device Fabrication* (Taylor&Franics Group)

[3] Puač N, Škoro N, Spasić K, Živković S, Milutinović M, Malović G, Petrović Z Lj 2017 *Plasma Process Polym*. **15** e1700082

[4] Lazović S, Puač N, Miletić M, Pavlica D, Jovanović M, Bugarski D, Mojsilović S, Maletić D, Malović G, Milenković P and Petrović Z Lj 2010 *New Journal of Physics* **12** 083037

[5] Puač N, Gherardi M, Shiratani M 2017*Plasma Process Polym*. e1700174

[6] Lisovskiy V A and Yegorenkov V D 1998 *J. Phys. D: Appl. Phys.* **31** 3349

[7] Gill E B W and von Engel A 1949 *Proc. R. Soc.* A **197** 107

[8] von Engel A 1965 *Ionized gases* (Oxford at the Clarendon Press)

[9] Phelps A V and Petrovic Z Lj 1999 *Plasma Sources Sci. Technol.* **8** R21

[10] Allis W P 1956 Motions of Ions and Electrons, ed. by Flugge S In: *Electron-Emission Gas Discharges I Encyclopedia of Physics* vol **21** (Springer Berlin Heidelberg) pp 383-444

[11] Allis W P and Brown C 1952 *Phys. Rev.* **87** 419

[12] MacDonald A D 1966 *Microwave Breakdown in Gases* (Wiley, New York)

[13] Morse P M, Allis W P and Lamar E S 1935 *Phys. Rev.* **48** 412

[14] Margenau H and Hartman L M 1948 *Phys. Rev.* **73** 309

[15] Holstein T 1946*Phys. Rev*. **70** 367

[16] Ginzburg V L and Gurevich A V 1960*Sov. Phys. Usp.***70** 393

[17] Wilhelm J and Winkler R 1969*Ann. Der Physik* **23** 28

[18] Goto N and Makabe T 1990*J. Phys. D* **23** 686

[19] Bzenic S, Petrovic Z Lj, Raspopovic Z and Makabe T 1999 *Jpn. J. Appl. Phys.***38** 6077

[20] Dujko S, White R D, Petrović Z Lj 2011 *IEEE Transactions on Plasma Sciences* **39** 2560

[21] White R D, Ness K F, Robson R E 2002 *Applied Surface Science* **192** 26

[22] Kihara T 1952 *Rev. Mod. Phys*. **24** 45

[23] Raizer Yu P, *Gas Discharge Physics*, Springer, Berlin, 1991

[24] Makabe T, Nakano N and Yamaguchi Y 1992 *Phys. Rev. A,* **45** 4 2520

[25] Klas M, Moravsky L, Matejček Š, Radjenović B and Radmilović-Radjenović M 2015 *J.Phys. D: Appl.Phys.***48** 405204

[26] Klas M, Matejčik Š, Morvasky L, Radjenović B and Radmilović-Radjenović M 2017 *EPL* **120** 25002

[27] Lee I, Graves D B and Lieberman *Plasma Sources Sci. Technol.* 2008 **17** 015018

[28] Kushner M J 2009 *J. Phys. D: Appl. Phys.* **42** 194013

[29] Donko Z 2011 *Plasma Sourc. Sci. and Tech.* **20** 024001

[30] Verboncoeur J P 2005 *Plasma Phys. Control. Fusion* **47** A231

[31] Birdsall C K and Langdon A B 1985 *Plasma Physics via Computer Simulation* (New York: McGraw-Hill)

[32] Birdsall C K 1991 *IEEE Trans. On Plasma Sci.* **19** 65

[33] Raspopovic Z M, Sakadzic S, Bzenic S A, Petrovic Z Lj 1999 *IEEE Trans. On Plasma Sci.* **27**1241

[34] Petrovic Z Lj, Raspopovic Z M, Dujko S and Makabe T 2002 *Appl. Surf. Sci.* **192** 1-25

[35] Savić M, Radmilovic-Radjenovic M, Šuvakov M, Marjanović S, Marić D, Petrović Z Lj 2011 *IEEE T Plasma Sci*. **39** 2556

[36] Šuvakov M, Ristivojević Z, Petrović Z Lj, Dujko S, Raspopović Z M, Dyatko N A, Napartovich A P 2005 *IEEE Trans. Plasma Sci*. **33** 532

[37] Ristivojevic Z, Petrovic Z Lj 2012 *Plasma Sources Sci. Tech.* **21** 035001

[38] Petrovic Z Lj, Bzenic S, Jovanovic J, Đurovic S 1995*J. Phys. D***28** 2287

[39] Petrović Z Lj, Šuvakov M, Nikitović Ž, Dujko S, Šašić O, Jovanović J, Malović G and Stojanović V 2007 *Plasma Sources Sci. Technol*. **16** S1-S12

[40] Phelps A V, http://www.jila.colorado.edu/avp/collision_data/electronneutral/

[41] Korolov I, Derzsi A and Donko Z 2014 *J.Phys.D:Appl.Phys*. **47** 475202

[42] Korolov I, Donko Z 2015 *Phys. of Plasmas* **22** 093501

[43] Lisovkiy V, Booth J-P, Landry K, Douai D, Cassagne V and Yegorenkov V 2006 *J. Phys. D:Appl Phys.* **39** 660

[44] Francis G 1956 *Gas Discharges II* In: Encyclopedia of physicsed. By Flugge S **XXII** (Springer-Verlag, Berlin)

[45] Lisovskiy V, Booth J-P, Landry K, Douai D, Cassagne V, Yegorenkov V 2008 *EPL* **82** 15001